Three-Dimensional Particle Simulations of Electron Extraction for a Miniature Microwave Discharge Neutralizer Using Water as the Propellant

IEPC-2019-154

Presented at the 36th International Electric Propulsion Conference
University of Vienna • Vienna, Austria
September 15-20, 2019

Yosuke Sato[1] and Kengo Nakamura[2]
Yokohama National University, Yokohama, 240-8501, Japan

Hiroyuki Koizumi[3]
The University of Tokyo, Kashiwa, 277-8561, Japan

and

Yoshinori Takao[4]
Yokohama National University, Yokohama, 240-8501, Japan

Abstract: We have conducted three-dimensional particle simulations for a miniature microwave discharge water neutralizer in order to analyze the dependence of the magnetic fields on the discharge characteristics and an electron extraction efficiency. We change the conventional magnetic field configuration to an improved one whose magnetic field lines pass through the entire orifice region in order to enhance the electron extraction along them. The simulation results indicate that distributions of the electron density and the positive ion density appear along the magnetic field lines passing through the electron cyclotron resonance area, whereas the negative ion density distributes along with the potential distribution in each magnetic field. In addition, the electron extraction efficiency in the improved magnetic field is increased by about 1.8 times comparing that in the conventional magnetic field.

Nomenclature

B_{ST}	=	magnetostatic field
L_{inside}	=	electron loss ratio toward the inside wall of the discharge chamber
$L_{outside}$	=	electron loss ratio toward the outside wall of the discharge chamber
n_e	=	electron density
n_+	=	total positive ion density
n_-	=	total negative ion density
P_{abs}	=	absorbed power
Δt_{EM}	=	time increment for microwave electromagnetic fields
Δt_e	=	time increment for electrons
Δt_i	=	time increment for ions

[1] Graduate Student, Department of Mechanical Engineering, Materials Science, and Ocean Engineering, sato-yosuke-st@ynu.jp.
[2] Graduate Student, Department of Systems Integration.
[3] Associate Professor, Department of Advanced Energy.
[4] Associate Professor, Division of Systems Research, takao@ynu.ac.jp.

η_{ext} = electron extraction efficiency
φ = potential

I.Introduction

SINCE 2013, the number of launched microspacecraft has been increasing drastically. Even universities and small companies can develop microspacecraft because of the low costs and short development periods.[1] Moreover, advanced missions, such as deep space exploration, have also been increasing.[2] For such advanced missions, propulsion systems are indispensable for microspacecraft in order to change their orbit arbitrary. However, microspacecraft have a severe limitation on the size and power consumption. Hence, in order to mount propulsion systems on microspacecraft, propulsion systems have to be miniaturized and their power consumption should be saved. One of the propulsion systems for microspacecraft is an ion thruster which can achieve high delta-*v*, and the research of a Miniature Ion Propulsion System (MIPS) has been conducted in Japan.[3,4] The MIPS employs electron cyclotron resonance (ECR) discharges with ring-shaped permanent magnets and microwave antenna for its ion source and neutralizer. The MIPS was mounted on a 50-kg-class spacecraft and operated in space successfully for the first time in the world.[5] In addition, since the demand for 10-kg-class spacecraft is increasing in recent years, propulsion systems for them have also been developed. However, the MIPS has a bulky gas tank to reserve xenon, which accounts for 40% of its total weight.[5] Thus, removing the gas tank is effective for further miniaturization of the MIPS. Here, we have proposed an ion thruster using water as a liquid propellant[6,7] based on the MIPS because water can be reserved without the gas tank and handled easily. Although water causes oxidation of a hollow cathode or electrodes, it is not a critical issue for the water ion thruster because the thruster employs ECR discharge, which does not use a hollow cathode or electrodes, for its ion source and neutralizer.

The water ion thruster was already operated on the ground and measured its thrust performance by the University of Tokyo.[8] In addition, in previous studies, we have been conducted three-dimensional (3D) particle simulations for the plasma source of the water ion thruster[9,10] because experimental measurements of discharge characteristics were difficult due to the small size of the discharge chamber. On the other hand, the water neutralizer has not been investigated numerically even though its performance is also associated with the water ion thruster performance. Moreover, it is expected that the performance of the water neutralizer is lower than that of the xenon neutralizer because of the negative ions, dissociation reaction, ionization collision cross sections, and so on. Hence, it is essential to improve the performance of the water neutralizer to develop the water ion thruster which can accomplish advanced missions. However, it is difficult to improve the water neutralizer performance due to the complexity of water plasma. Therefore, we attempt to improve the water neutralizer performance by applying conditions which can improve the xenon neutralizer performance since configurations of the water and xenon neutralizer are the same. In our previous study of the xenon neutralizer, it was elucidated that the electron extraction depends on both the motion along magnetic field lines and the $\boldsymbol{E} \times \boldsymbol{B}$ drift.[11] Moreover, changing the magnetic field, the performance of the xenon neutralizer was increased by about 1.5 times. Hence, we analyzed the effects of the magnetic field configurations on the discharge characteristics and performance of the water neutralizer using 3D particle simulations.

II.Numerical Model

We employed 3D particle simulations which consist of a Particle-in-Cell calculation with a Monte Carlo collisions algorithm (PIC–MCC) for the kinetics of charged particles, a Finite-Difference Time-Domain (FDTD) algorithm for the electromagnetic fields of microwaves, and a finite element analysis using ANSYS Emag™ software for the magnetostatic fields of permanent magnets. In addition, the null-collision method in MCC was used for reducing the calculation time.[12] We took into account the following species as particles: H_2O^+, OH^+, and H^+ positive ions, H^-, O^-, and OH^- negative ions, and electrons. In addition, the simulations were based on the following assumptions: (i) Neutral particles are spatially and temporally uniform with a Maxwellian distribution at a gas temperature

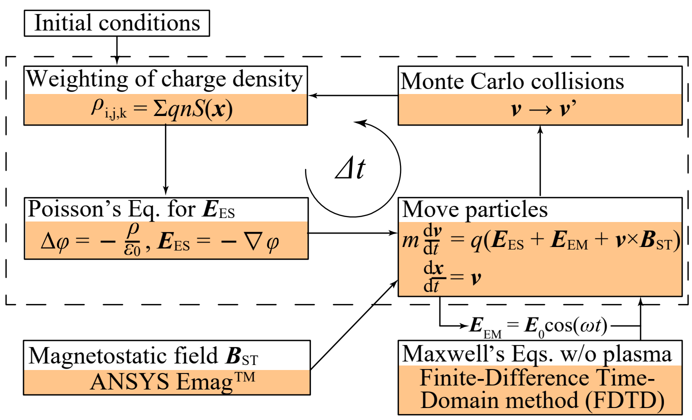

Figure 1. Calculation flow of the PIC–MCC simulation.

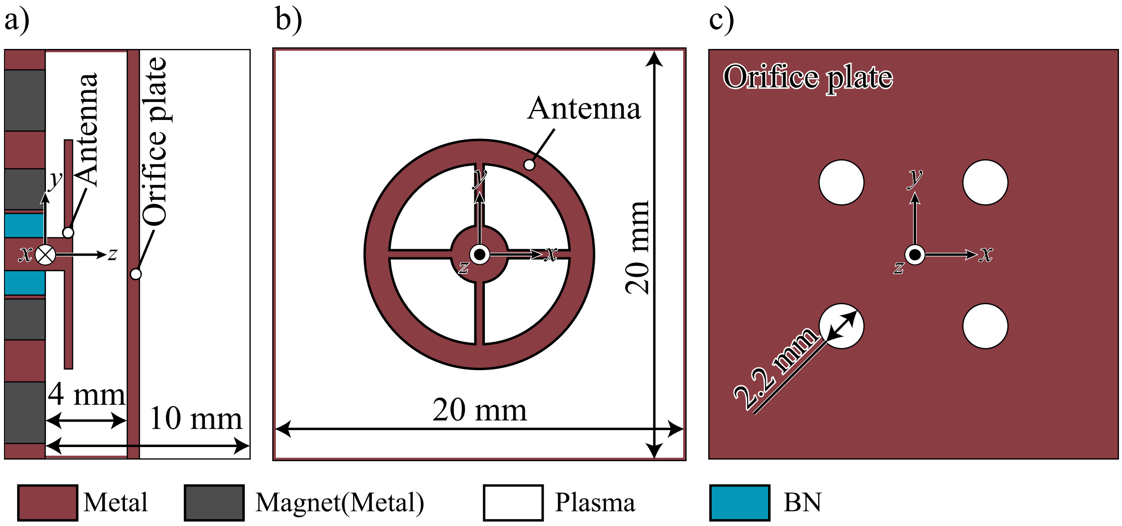

Figure 2. Schematic of the calculation model: (a) *z-y* plane at *x* = 0 mm, (b) *x-y* plane at the antenna position, and (c) *x-y* plane at *z* = 4.0 mm.

of 300 K in the plasma region. (ii) The magnetic fields of microwaves are negligibly small compared to the magnetostatic fields $\boldsymbol{B}_{ST}$. (iii) The motion of excited-state atoms is not considered. (iv) Coulomb collisions are not taken into account. (v) Since the power of microwaves is low in this simulation, the plasma current is neglected. The calculation model is briefly described below because conditions are basically the same as that employed in our previous paper.[10]

A. Calculation Flow

Figure 1 shows a flow chart of the simulation employed in this work. First, we set initial conditions and then we solved Maxwell's equations by FDTD for the electromagnetic fields of microwaves with a time increment $\Delta t_{EM} = 1.49 \times 10^{-13}$ s (1/1600 of a microwave cycle for 4.2 GHz) to obtain a steady-state electromagnetic configuration without plasma. Second, we conducted electrostatic PIC–MCC simulation using the time-varying electric field of microwaves calculated by FDTD, the electrostatic electric field of plasma, and the magnetic fields produced by permanent magnets. In the simulation, the power absorbed in the plasma P_{abs} = 2.0 W was used as an input parameter, where P_{abs} was obtained by calculating the change in kinetic energy of electrons and ions. Last, we modified the amplitude of electromagnetic fields to conform P_{abs} to 2.0 W. The above procedure was iterated until the steady-state solution was obtained.

B. Configuration

Figure 2 shows the calculation model of the neutralizer. The calculation domain consists of a 20 mm × 20 mm × 4 mm, a 0.6-mm thickness orifice plate which has four circular orifices for the electron extraction, and 20 mm × 20 mm × 5.4 mm region for investigation of the electron extraction. The potential on walls was set at zero, and the potential at z = 10 mm was set at 20 V for the electron extraction voltage. Figure 3 shows the conventional and improved magnetic fields, which are referred to as MF-1 and MF-2, respectively. The size of the ring-shaped magnets in MF-1 is the same as the previous paper.[10] In MF-2, we changed the outside diameter of the inner ring-shaped magnet (from 8 to 6 mm) in order to enhance the electron extraction along magnetic field lines by forming magnetic field lines passing through the entire

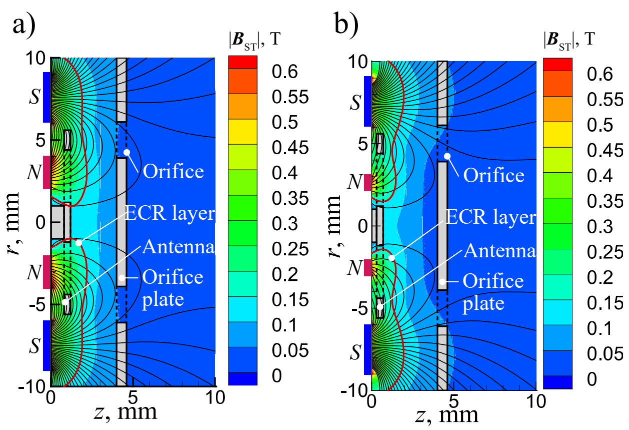

Figure 3. Contour plots of the magnetic fields of (a) MF-1 and (b) MF-2 for the *z-r* plane, together with the thick red lines representing the resonant magnetic field of 0.15 T for 4.2-GHz microwave.

orifice region. In addition, the gap distance from the magnet surface to the antenna was also reduced so that the ECR layer is not too close to the antenna. Changing the magnetic field of the xenon neutralizer to MF-2, an electron extraction efficiency η_{ext}, which was defined as a ratio of extracted electron current against generated electrons per unit time, was increased by about 1.5 times. Thus, it can be expected that the electron extraction efficiency of the water neutralizer is also improved as with the case of the xenon neutralizer.

C. Additional Remarks

The grid spacing in the PIC–MCC simulation was set at 0.1 mm, and the microwave frequency was set at 4.2 GHz. Time steps for PIC were $\Delta t_e = 5.95 \times 10^{-12}$ s (1/40 of a microwave cycle) for electrons and $\Delta t_i = 2.38 \times 10^{-12}$ s (one microwave cycle) for ions. Corresponding to a mass flow rate of 35 µg/s in the experiment, the neutral gas pressure in the plasma source was set at 6.3 mTorr. These calculation conditions are the same as those in our previous paper.[10] The results of the simulations were averaged over 50 000 microwave cycles.

III. Numerical Results and Discussion

Figure 4 shows the time-averaged distributions of the electron density n_e, the total positive ion density n_+, the total negative ion density n_-, and the potential φ for each magnetic field at the *z*-*y* plane, together with thick red lines which represent the resonant magnetic field of 0.15 T for 4.2 GHz microwave. From Figs. 4(a) and 4(e), a high electron density region appeared along the magnetic field lines passing through the ECR area in each magnetic field. In addition, the electron density in MF-2 reached a higher value than that in MF-1 because the mirror ratio of MF-2 was larger than that of MF-1, as implied in Fig. 3. As shown in Figs. 4(b) and 4(f), distributions of the positive ions formed almost the same distribution as those of the electrons. This is because a number of ionization collisions occurred in a high electron density region. On the other hand, the total negative ion density distributions, which were shown in Figs. 4(c) and 4(g), were distributed along with the potential distributions, which were shown in Figs. 4(d) and 4(h). These tendencies are the same as results of a simulation for the water plasma source.[10]

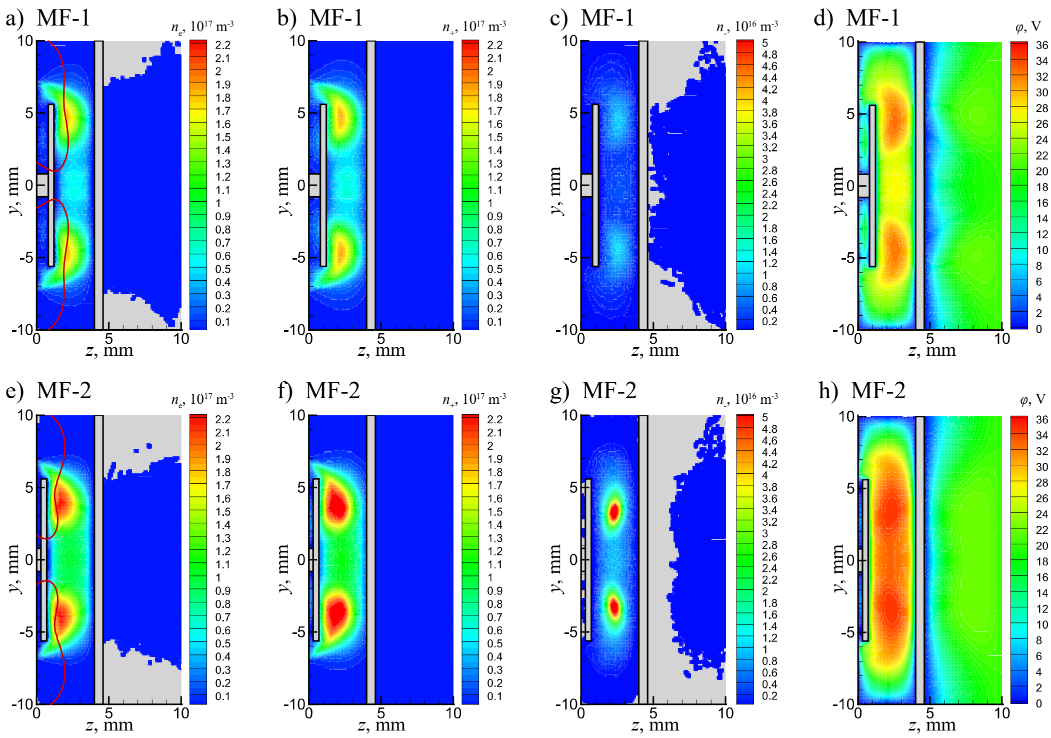

Figure 4. Time-averaged distributions of (a) the electron density, (b) the total positive ion density, (c) the total negative ion density, and (d) the potential for MF-1; and time-averaged distributions of (e) the electron density, (f) the total positive ion density, (g) the total negative ion density, and (h) the potential for MF-2 at the *z*-*y* plane. The thick red lines in (a) and (e) represent the resonant magnetic field of 0.15 T for 4.2-GHz microwave.

Table 1 shows electron loss ratio toward the inside wall of the discharge chamber L_{inside} and the outside wall of the discharge chamber $L_{outside}$ and the electron extraction efficiency η_{ext} for each magnetic field. The electron extraction efficiency in MF-2 was 18.2%, whereas that in MF-1 was about 9.5%. The increase in the efficiency was attributed to the great reduction of the electron loss toward the outside wall of the discharge chamber. Magnetic field lines of MF-1 passed the orifices and returned to the orifice plate as shown in Fig. 3(a). Therefore, a number of the electrons which passed through the orifices were lost toward the outside wall of the discharge chamber along these magnetic field lines. Contrarily, magnetic field lines of MF-2 passed the orifices and expanded along the *z*-axis as shown in Fig. 3(b). Thus, the electron loss toward the outside wall of the discharge chamber was suppressed. As a consequence of these mechanisms, it was elucidated that the shape of magnetic field lines outside the discharge chamber strongly affected the electron extraction efficiency, and the electron extraction efficiency was improved by changing magnetic fields from MF-1 to MF-2 as with the case of the xenon neutralizer.

Table 1. Electron loss ratio toward the inside and outside wall of the discharge chamber and the electron extraction efficiency.

	MF-1	MF-2
$L_{outside}$, %	6.61	1.38
L_{inside}, %	83.9	80.4
η_{ext}, %	9.52	18.2

IV.Conclusion

In this work, we employed 3D PIC–MCC simulation for a water ECR neutralizer in order to investigate the effect of the magnetic fields on the discharge characteristics and an electron extraction efficiency. We conducted the simulations for the conventional and an improved magnetic field, which are referred to as MF-1 and MF-2, respectively. In order to enhance the electron extraction along magnetic field lines, those of MF-2 passed through the entire orifice region. From the results, it was confirmed that the electron density distribution and the total positive ion density distribution appeared along the magnetic field lines passing through the ECR area in both MF-1 and MF-2, whereas the negative ions were distributed along with the potential distribution in both MF-1 and MF-2. With respect to the performance, changing the conventional magnetic field to the improved one, the electron extraction efficiency was increased by about 1.8 times, and it was indicated that the shape of magnetic field lines outside the discharge chamber strongly affected the electron extraction efficiency. On the other hand, the efficiency of the water neutralizer is still low, and further improvement is required. In future work, we will analyze mechanisms of an electron loss toward the inside wall of the discharge chamber, which occupied over 80% in each magnetic field configuration, in order to suppress the electron loss and improve the efficiency.

Acknowledgments

This work was partially supported by JSPS KAKENHI, Grant No. JP16H06370. It partly used computational resources under the Collaborative Research Project for Enhancing Performance of Programming by the Academic Center for Computing and Media Studies, Kyoto University. Part of the computer simulation was performed on a supercomputer at KDK computer system at the Research Institute for Sustainable Humanosphere, Kyoto University.

References

[1]SpaceWorks Enterprises, Inc., "Nano/Microsatellite Market Forecast 2019," URL: https://www.spaceworks.aero/wp-content/uploads/Nano-Microsatellite-Market-Forecast-9th-Edition-2019.pdf [cited 19 August 2019].

[2]Benedetti, G., Bloise, N., Boi, D., Caruso, F., Civita, A., Corpino, S., Garofalo, E., Governale, G., Mascolo, L., Mazzella, G., Quarata, M., Riccobono, D., Sacchiero, G., Teodonio, D., and Vernicari, M. P., "Interplanetary CubeSats for asteroid exploration: Mission analysis and design," *Acta Astronautica*, Vol. 154, 2019, pp. 238-255.

[3]Koizumi, H., Komurasaki, K., Aoyama, J., and Yamaguchi, K., "Engineering Model of the Miniature Ion Propulsion System for the Nano-satellite: HODOYOSHI-4," *Trans. JSASS Aerospace Tech. Japan*, Vol. 12, No. ists29, 2014, Tb_19-Tb_24.

[4]Koizumi, H., Komurasaki, K., Aoyama, J., and Yamaguchi, K., "Development and Flight Operation of a Miniature Ion Propulsion System," *J. Propul. Power*, Vol. 34, No. 4, 2017, pp. 960-968.

[5]Koizumi, H., Kawahara, H., Yaginuma, K., Asakawa, J., Nakagawa, Y., Nakamura, Y., Kojima, S., Matsuguma, T., Funase, R., Nakatsuka, J., and Komurasaki, K., "Initial Flight Operations of the Miniature Propulsion System Installed on Small Space Probe," *Trans. JSASS Aerospace Technology Japan*, Vol. 14, No. ists30, 2016, pp. Pb_13-Pb_22.

[6]Nakagawa, Y., Kawahara, H., Koizumi, H., and Komurasaki, K., "Fundamental Experiments with Liquid Propellants for the Microwave-discharge Ion Thruster," Space Propulsion 2016, Roma, Italy, 2016, SP2016-312540.

[7]Nakagawa, Y., Koizumi, H., Kawahara, H., and Komurasaki, K., "Performance characterization of a miniature microwave discharge ion thruster operated with water," *Acta Astronautica*, Vol. 157, 2019, pp. 294-299.

[8]Nakagawa, Y., Tomita, D, Koizumi, H., and Komurasaku, K., "Design and Test of a 100 µN-class Thrust Stand for a Miniature Water Ion Thruster with CubeSat," *Trans. JSASS Aerospace Technology Japan*, Vol. 16, No. 7, 2018, pp. 673-678.

[9]Nakamura, K., Nakagawa, Y., Hiroyuki, K., and Takao, Y., "Numerical Analysis of a Miniature Microwave-discharge Ion Thruster Using Water as the Propellant," *Trans. Japan Soc. Aero. Space Sci.*, Vol. 61, No. 4, 2018, pp.152-159.

[10]Nakamura, K., Koizumi, H., Nakano, M., and Takao, Y., "Effects of negative ions on discharge characteristics of water plasma source for a miniature microwave discharge ion thruster," *Phys. Plasmas*, Vol. 26, No. 4, 2019, pp. 043508-1-10.

[11]Hiramoto, K., Nakagawa, Y., Koizumi, H., and Takao, Y. "Effects of E×B drift on electron transport across the magnetic field in a miniature microwave discharge neutralizer," *Phys. Plasmas*, Vol. 24, No. 6, 2017, pp.064504-1-5.

[12]Vahedi, V. and Surendra, M., "A Monte Carlo collision model for the particle-in-cell method: applications to argon and oxygen discharges," *Comput. Phys. Commun*., Vol. 87, No. 1-2, 1995, pp. 179-198.